The Astrophysical Journal, 623:889–896, 2005 April 20

ATOMIC CARBON IN THE SOUTHERN MILKY WAY

Tomoharu Oka,[1] Kazuhisa Kamegai,[1,2] Masaaki Hayashida,[1] Makoto Nagai,[1] Masafumi Ikeda,[3,4] Nobuyuki Kuboi,[1] Kunihiko Tanaka,[1] Leonardo Bronfman,[5] and Satoshi Yamamoto[1]

Received 2004 May 31; accepted 2005 January 6

ABSTRACT

We present a coarsely sampled longitude-velocity (*l-V*) map of the region $l = 300^\circ$–354°, $b = 0^\circ$ in the 492 GHz fine-structure transition of neutral atomic carbon ($C^0\ ^3P_1$–$^3P_0$; [C I]), observed with the Portable 18 cm Submillimeter-wave Telescope (POST18). The *l-V* distribution of the [C I] emission resembles closely that of the CO $J = 1$–0 emission, showing a widespread distribution of atomic carbon on the Galactic scale. The ratio of the antenna temperatures, $R_{\mathrm{C\ I/CO}}$, concentrates on the narrow range from 0.05 to 0.3. A large velocity gradient (LVG) analysis shows that the [C I] emission from the Galactic disk is dominated by a population of neutral gas with high C^0/CO abundance ratios and moderate column densities, which can be categorized as diffuse translucent clouds. The ratio of bulk emissivity, $J_{\mathrm{C\ I}}/J_{\mathrm{CO}}$, shows a systematic trend, suggesting the bulk C^0/CO abundance ratio increasing with the Galactic radius. A mechanism related to kiloparsec-scale structure of the Galaxy may control the bulk C^0/CO abundance ratio in the Galactic disk. Two groups of high-ratio ($R_{\mathrm{C\ I/CO}} > 0.3$) areas reside in the *l-V* loci several degrees inside of tangential points of the Galactic spiral arms. These could be gas condensations just accumulated in the potential well of spiral arms and be in the early stages of molecular cloud formation.

Subject headings: Galaxy: structure — ISM: abundances — ISM: atoms

1. INTRODUCTION

Since the first detection of the CO $J = 1$–0 line (Wilson et al. 1970), it has been a principal tool used to study the molecular component in the Milky Way and external galaxies. Large-scale CO surveys (e.g., Gordon & Burton 1976; Sanders et al. 1984; Dame et al. 1986, 1987; Bronfman et al. 1988, 1989) have shown that most of the molecular material in the Galaxy is contained in the form of molecular clouds, which are sites of star formation. The Galactic distribution of molecular clouds is characterized by their concentration in the Galactic center region and in a "ring" at a galactocentric radius of 0.4–0.8 $R_\odot$, in sharp contrast to the flatter distribution of atomic hydrogen. In addition, giant molecular clouds and their complexes are concentrated to spiral arms in the Galactic disk (e.g., Sanders et al. 1985; Stark et al. 1987). These indicate that formation processes of molecular clouds must be closely related to the kiloparsec-scale structure of the Galaxy.

To investigate formation processes of molecular clouds, it is crucial to know the large-scale spatial distribution and kinematics of molecular cloud-forming regions in the Galaxy. First and foremost, direct detections of such regions must be essential. Neutral atomic carbon (C^0) is the most promising tool to trace cloud-forming regions, since the conversion timescale of C^0 into CO is comparable to the dynamical timescale of molecular clouds. Chemical models predict that C^0 becomes abundant, when it has not been converted into CO, in the early stage of chemical evolution of a molecular cloud (e.g., Suzuki et al. 1992). The fine-structure $^3P_1$–$^3P_0$ transition of atomic carbon ([C I] 492.160651 GHz) must be a superior tracer of C^0 in interstellar space, since it is easily excited at densities $n(\mathrm{H_2}) \gtrsim 10^3$ cm^{-3} and kinetic temperatures $T_k \gtrsim 20$ K. Recently, an extensive survey of nearby molecular clouds in the [C I] 492 GHz line with the Mount Fuji submillimeter-wave telescope found such molecular clouds in the early stage of chemical evolution (Maezawa et al. 1999; Kamegai et al. 2003; Oka et al. 2004). However, the sky coverage of the Mount Fuji telescope survey is still limited ($\sim$50 deg^2), since its beam size (2.′6 at 492 GHz) is too small to survey the whole Galaxy.

For the exclusive use of the wide-angle survey of the Milky Way in the $C^0\ ^3P_1$–$^3P_0$ line, we have developed a very small submillimeter-wave telescope, the Portable 18 cm Submillimeter-wave Telescope (POST18). This paper presents a brief description of POST18 as well as the results from a pilot survey of the Milky Way in the [C I] 492 GHz line. In this paper we adopt the Galactic constants $r_\odot = 8.5$ kpc and $\Theta_\odot = 220$ km s^{-1}, following the recommendation by the IAU in 1985.

2. INSTRUMENT

A schematic drawing of the telescope is shown in Figure 1. The telescope is designed to be compact for portability. The total weight of the telescope, including the receiver, back end, and control system, is approximately 200 kg.

The telescope has an offset paraboloidal main reflector with a diameter of 18 cm that gives a beamwidth of 13.′6 at 492 GHz. An optical telescope is attached to the edge of the main reflector to measure the instrumental pointing errors. The beam from the main reflector is dropped by a flat subreflector, being directed to the mixer horn in the Dewar. Two equal harmonic drive motors are used to drive azimuth (Az) and elevation (El) axes. The torque of the motors is 1.5 Nm, and the maximum angular

[1] Research Center for the Early Universe and Department of Physics, University of Tokyo, 7-3-1 Hongo, Bunkyo-ku, Tokyo 113-0033, Japan; tomo@phys.s.u-tokyo.ac.jp.
[2] Institute of Astronomy, University of Tokyo, 2-21-1 Osawa, Mitaka, Tokyo 181-0015, Japan.
[3] National Astronomical Observatory of Japan, 2-21-1 Osawa, Mitaka, Tokyo 181-8588, Japan.
[4] Computational Science Division, Advanced Computing Center, Institute of Physical and Chemical Research (RIKEN), 2-1 Hirosawa, Wako, Saitama 351-0198, Japan.
[5] Departamento de Astronomía, Universidad de Chile, Casilla 36-D, Santiago, Chile.

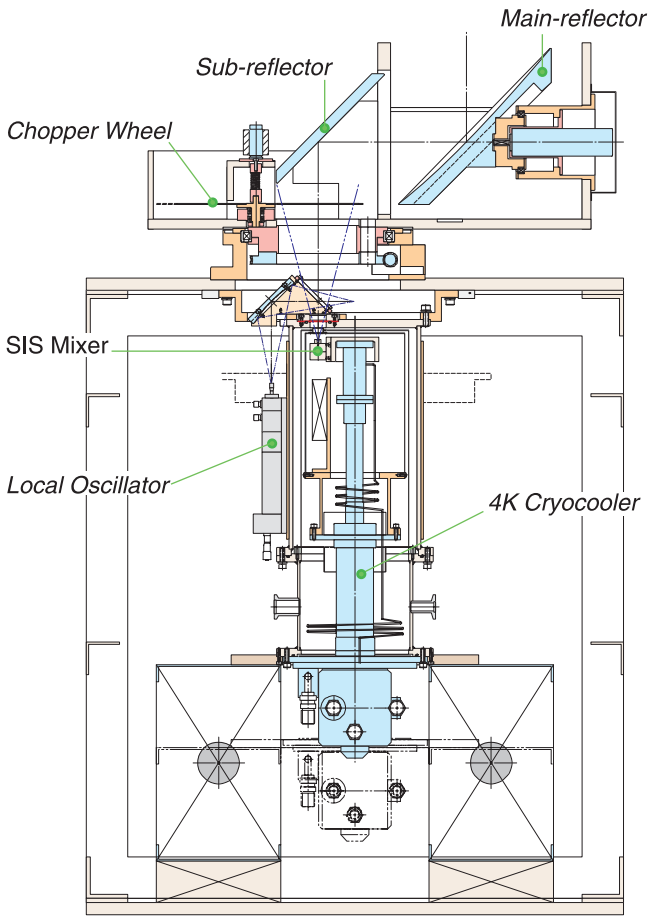

FIG. 1.—Schematic drawing of the Portable 18 cm Submillimeter-wave Telescope.

speed is 4200 revolutions per minute (rpm). Rotations of the motors are decelerated by 100:1 and 50:1 in Az and El, respectively, and the Az axis is driven via a 160:1 worm gear.

We developed a superconductor-insulator-superconductor (SIS) mixer receiver for the 500 GHz band. We employed a Nb-based parallel connected twin junction (PCTJ) type mixer that was fabricated at the Nobeyama Radio Observatory (NRO). The mixer is operated in the double-sideband (DSB) mode, and the 492 GHz signal is received in the lower sideband. The intermediate frequency (IF) is 1.8–2.5 GHz. The receiver employs a two-stage Gifford-MacMahon cryocooler (Sumitomo RD101), which has a cooling capacity of 0.1 W on the 4 K cold stage with a 1.5 kW power consumption. The local oscillator (LO) signal is generated by multiplying the output of a W-band (~80 GHz) Gunn diode oscillator with a 2×3 multiplier (Radiometer Physics GmbH). The LO signal is quasi-optically coupled to the radio frequency (RF) signal by a free-standing wire grid equipped on the top of the Dewar. The IF signal from the mixer is amplified by a cooled low-noise amplifier (LNA; Nitsuki model 9838S4). The DSB receiver noise temperature including LNA was $T_{\rm RX} \simeq 140$ K in the laboratory.

The IF signal from the Dewar is amplified by +66 dB at room temperature and is fed into a wideband acousto-optical spectrometer (AOS). The imaging optics enables us to cover 900 MHz bandwidth with a 1728 channel charge-coupled device (CCD) array. The effective frequency resolution of the spectrometer is 1.0 MHz. The frame rate of the CCD was set to 4 ms. The gain variation of a spectrum obtained with the AOS is less than a 3 dB peak-to-peak variation over 700 MHz.

TABLE 1
THE PARAMETERS OF POST18 AT 492 GHz

Parameter	Value
Main Reflector	
Optics	Offset paraboloid
Diameter	18 cm
Focal length	420 mm
HPBW	13.′6
Receiver	
Cryocooler	Two-stage GM
Mixer type	SIS PCTJ
IF frequency	1.8–2.5 GHz
Receiver temperature	140 K (DSB)
Spectrometer	
Type	AOS
Channel number	1728 ch
Bandwidth	700 MHz (430 km s^{-1})
Resolution	1.0 MHz (0.6 km s^{-1})

All instruments are controlled by a personal computer via GP-IB and digital I/O interfaces. The operating system of the computer is Windows 2000. The telescope control software has been developed with the Visual C++ package. The parameters of the telescope are listed in Table 1.

3. OBSERVATIONS

On 2003 September 4, the telescope was assembled at the site of the Atacama Submillimeter-wave Telescope Experiment (ASTE) at Pampa la Bola (altitude 4840 m), Chile. The electric power was supplied from the ASTE power plant. The telescope needs about a week for installation and adjustment. The instrumental pointing errors were corrected by observing stars with the optical telescope. The pointing errors of the radio axis are measured by observing continuum emission from the Sun, maintained to 75″ in rms. The beam efficiency was estimated by observing the new Moon to be $\eta_{\rm Moon} = 85\% \pm 4\%$ by assuming the brightness temperature of the new Moon to be 110 K (brightness at $\lambda = 1$ mm; Linsky 1973). We successfully operated the telescope from September 10 to 30 and from November 15 to December 4 in 2003.

The atmospheric opacity was measured by tipping the main reflector around the El axis. The zenith opacity at 492/496 GHz was from 0.5 to 1.0 during the operation. Atmosphere-corrected system temperatures ranged from 600 to 1000 K in DSB. The observations were made using position switching to reference positions ~2° off the Galactic equator and less than 2.°5 apart in longitude. The reference positions were selected in emission-free regions of deep CO maps (Bronfman et al. 1989). The data were calibrated by the standard chopper-wheel method (Ulich & Haas 1976). The intensity reproducibility was checked by observing the same position in the ρ Oph cloud and was found to be stable within ±15% in rms.

The very dry submillimeter sky at the Pampa la Bola site enables us to detect faint [C I] line emission from the Galactic plane. A total of 55 sparsely sampled spectra were obtained in the region $l = 300°-354°$, $b = 0°$, with a spacing of $\Delta l = 1°$. A test for the feasibility of detecting Galactic-scale variations from coarsely sampled data has been performed in the case of CO by Liszt (1993). He concluded that there is no severe penalty

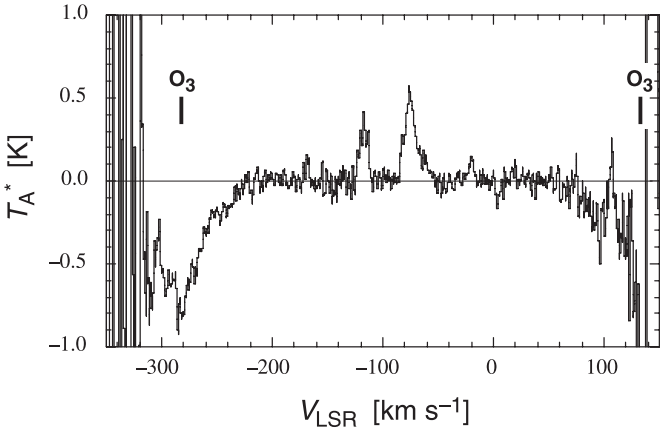

FIG. 2.—Typical [C I] spectrum in the Galactic plane at $l = 330°$. Broad absorption features centered at $V_{LSR} \sim -280$ and +130 km s^{-1} are telluric ozone lines at 496.254 GHz (USB interference) and 491.951 GHz, respectively.

due to sampling in a limited fashion in order to detect the Galactic-scale behavior of emissivity. A typical [C I] spectrum is shown in Figure 2. The bandwidth and resolution of the back end corresponds to a 400 km s^{-1} velocity coverage and 0.6 km s^{-1} velocity resolution, respectively. However, strong interference of telluric ozone lines (496.254 and 491.951 GHz) reduces available bandwidth to as narrow as 300 km s^{-1}. Typical 600 s on-source integrations resulted in spectra having a noise level of $\Delta T_A^* \leq 0.1$ K in rms. The standard processed spectra have offsets from zero and the shape of the band characteristic curve of the back-end system because of the difference between the on/off continuum levels and the minimal nonlinearity in the back end. Thus, we subtracted baselines of the spectra by fitting fourth-order polynomial lines and the band characteristic curve of the back-end system.

4. RESULTS

We detected [C I] 492 GHz emission in about 90% of positions observed. Figure 3*a* shows a longitude-velocity (*l*-*V*) map of the southern Milky Way in the [C I] 492 GHz emission. The [C I] emission is generally weak, $T_A^* \leq 0.5$ K, over the *l*-*V* space we covered. The [C I] antenna temperature reaches $T_A^* \simeq 0.5$ K at only two positions, $(l, V_{LSR}) = (337°, -76$ km s$^{-1})$ and $(338°, -47$ km s$^{-1})$, where giant H II region complexes are associated (e.g., Georgelin & Georgelin 1976).

To compare the molecular and atomic phases of interstellar carbon, we have extracted CO $J = 1$–0 spectra from the large-scale survey data obtained with the Columbia–Universidad de Chile 1.2 m Millimeter-Wave Telescope (Bronfman et al. 1988, 1989; Bitran et al. 1997), which have the same positions and a similar angular resolution ($\simeq 9'$) as the [C I] data. Figure 3*b* shows a *l*-*V* map in the CO $J = 1$–0 emission. Loci in *l*-*V* space of three major spiral arms as well as the *l*-*V* track of the 3 kpc arm (Mulder & Liem 1986) are superposed. The three major spiral arms are modeled by usual logarithmic spirals, $r(\phi) = r_0 \exp(-p\phi)$ (e.g., Kennicutt 1982 and references therein). We calculated the parameters r_0, p by fitting log spirals to (r, ϕ) loci of giant H II regions ("bright" and "medium" in Georgelin & Georgelin 1976). The *l*-*V* maps show striking similarity; intense emission from molecular clouds that belong to the Norma and Scutum-Crux arms, lack of emission from the Sagittarius-Carina arm, and faint emission possibly associated with the 3 kpc arm. The lack of emission from the Sagittarius-Carina arm is most probably due to the large angular width of the arm, several

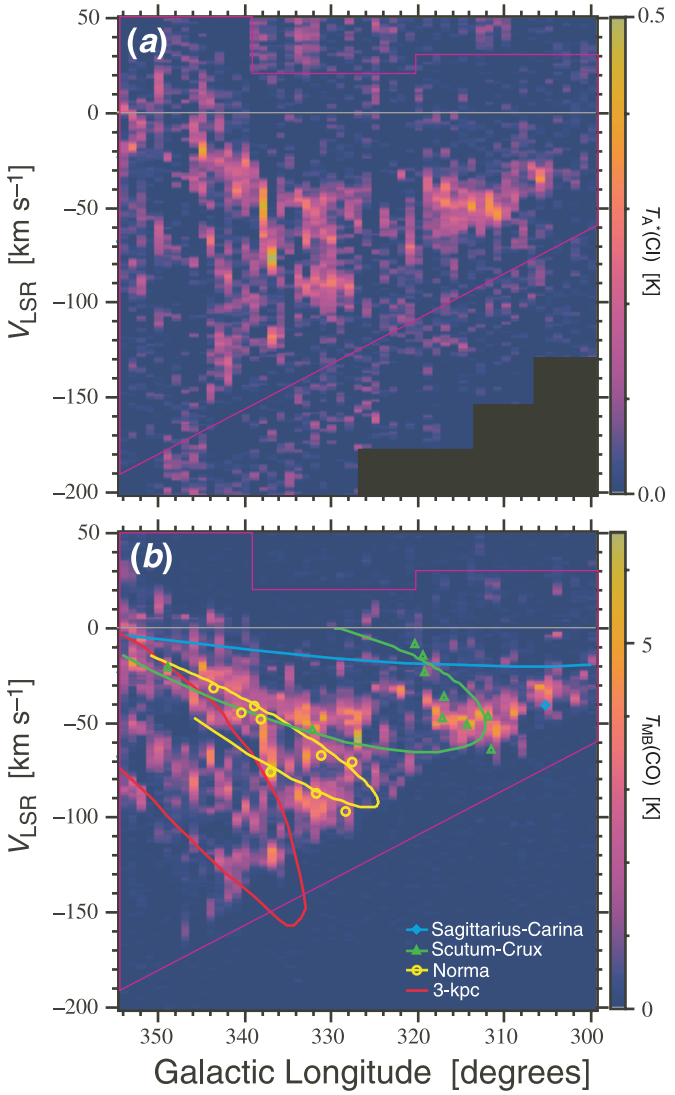

FIG. 3.—(*a*) Longitude-velocity map for [C I] 492 GHz emission, and (*b*) the corresponding map for CO $J = 1$–0 emission. Loci in *l*-*V* space of three major spiral arms and the 3 kpc arm (Mulder & Liem 1986) are shown by solid lines. Open polygons and circles show giant H II regions ("bright" and "medium" in Georgelin & Georgelin 1976). The data inside of the purple solid frame are used in the analyses.

degrees, being so near (∼1.5 kpc) and the sampling being restricted to $b = 0°$.

5. DISCUSSION

5.1. *Physical Conditions*

5.1.1. *Intensity Correlation and Ratio*

Intensity correlation plots may be useful to compare observed lines and to infer physical and chemical conditions of line-emitting gas. Figure 4 is the plot of T_{MB}(C I) versus T_{MB}(CO) made with the data in the *l*-*V* area indicated with the solid line in Figure 3. The following analyses use the same data set. A rough, linear correlation is apparent. Fitting the data to a straight line gives $T_{MB}(\text{C I}) = -0.01 + 0.12 T_{MB}(\text{CO})$, with a correlation coefficient $\rho = 0.75$. The linear correlation may suggest that both lines arise from the same population of interstellar matter.

To quantify the frequency distribution of the intensity ratio, $R_{\text{C I/CO}} \equiv T_{MB}(\text{C I})/T_{MB}(\text{CO})$, we made a histogram of the ratio (Fig. 5). Each column shows the sum of [C I] line intensity for data with $R_{\text{C I/CO}}$ in each bin. Since [C I] line is considered to be

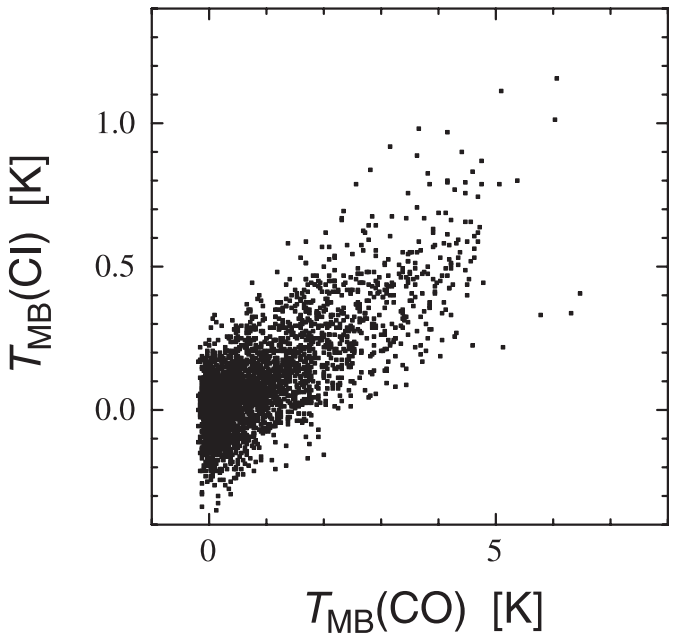

FIG. 4.—Plot of [C I] 492 GHz against CO $J = 1-0$ main-beam temperatures (T_{MB}). Both data sets were smoothed to a 2 km s^{-1} resolution.

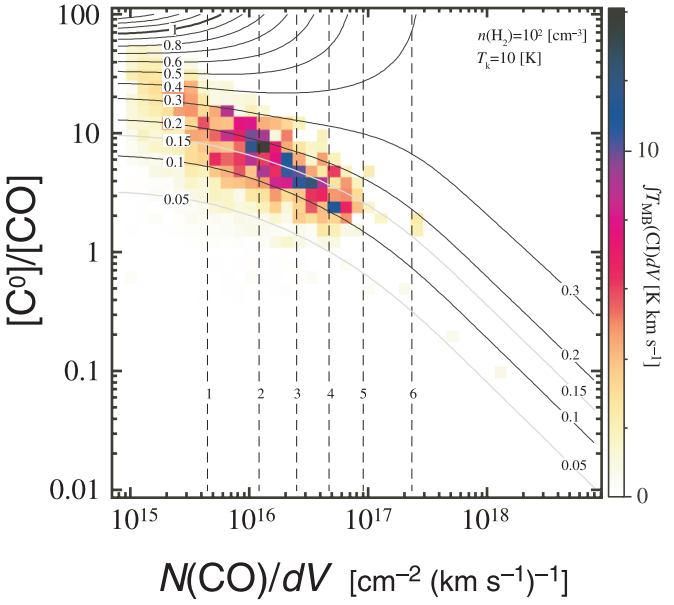

FIG. 6.—Calculated curves of constant [C I]/CO $J = 1-0$ intensity ratios (*solid lines*) and CO $J = 1-0$ intensities (*dashed lines*) as a function of CO column density per unit velocity width and C^0/CO abundance. Kinetic temperature is assumed to be 10 K and hydrogen density to be 10^2 cm^{-3}. The color map shows density distribution of observed data weighted by [C I] intensity.

fairly optically thin (e.g., Oka et al. 2001, 2004), the vertical axis may represent the amount of C^0 gas with a given $R_{C\,I/CO}$. The distribution of $R_{C\,I/CO}$ has a prominent peak at $\simeq$0.12. About 70% of [C I] emission comes from gas with $R_{C\,I/CO}$ between 0.05 and 0.3. This implies that [C I] emission from the Galactic disk may be dominated by a population of neutral interstellar matter with a specific physical condition.

The ratio of total integrated intensities, $W_{C\,I}/W_{CO}$, was 0.105 ± 0.004. Coarse resolution (7°) data by *COBE* gives a little higher value, $W_{C\,I}/W_{CO} = 0.18$. The discrepancy between *COBE* data and ours could arise from the incompleteness of our [C I] data set, implying that neutral gas with low $R_{C\,I/CO}$ may be abundant in the midplane of the Galactic disk compared to out of the plane. The results from the Antarctic Submillimeter Telescope and Remote Observatory (AST/RO) reported $R_{C\,I/CO}$ around 0.1 for gas in the Galactic center and 0.3–0.4 for gas in the foreground (Ojha et al. 2001). High-ratio gas in the foreground of the Galactic center could be in a conditionthat is not average in the Galactic disk. Observations of nearby external galaxies have shown that $R_{C\,I/CO}$ varies within galaxies or between galaxies (Gerin & Phillips 2000). They found that some galaxies show lower $R_{C\,I/CO}$ in the nucleus than in the disk. Our Galaxy seems to have no significant difference in $R_{C\,I/CO}$ between the nucleus and the disk, however.

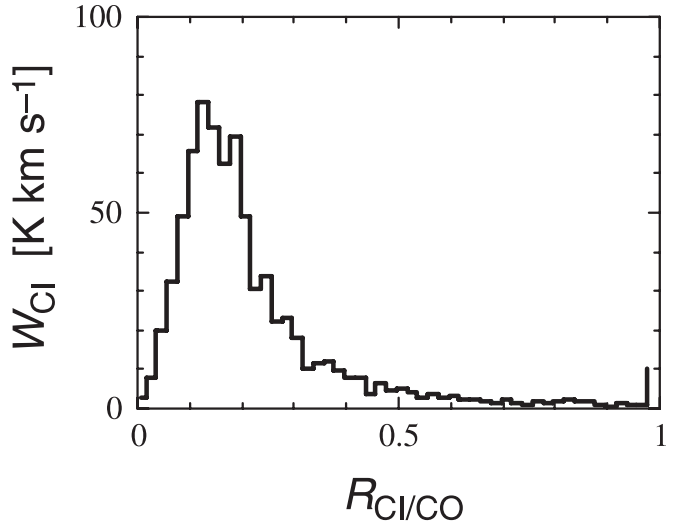

FIG. 5.—Binned distribution of intensity ratios, $R_{C\,I/CO} \equiv T_{MB}(C\,I)/T_{MB}(CO)$, weighted by [C I] intensity.

5.1.2. *LVG Analyses*

It is difficult, in general, to diagnose physical conditions of [C I]-emitting gas solely from the [C I]/CO intensity ratio $R_{C\,I/CO}$, since a number of parameters including excitation conditions and the ultraviolet radiation field affect $R_{C\,I/CO}$. In addition, different conditions sometimes result in similar values of $R_{C\,I/CO}$ (i.e., gas in the Galactic center and the disk). To avoid complication, we restrict our discussion to the variation in the Galactic disk, in which the environment is considered to be roughly uniform. We assume a constant density and a constant kinetic temperature in referring to the results of large velocity gradient (LVG) model calculations. Under these assumptions, $R_{C\,I/CO}$ is determined by the C^0/CO abundance ratio and the gas column density per velocity width: the higher abundance ratio gives the higher $R_{C\,I/CO}$, and the higher gas column density gives the higher $R_{C\,I/CO}$ if the C^0/CO abundance ratio is not unnaturally high, since the [C I] line is generally less opaque while the CO line easily saturates (see Fig. 6).

It is usually understood that the vast majority of molecular emission from the Galactic disk arises from material at $T_k <$ 15 K. The large-scale CO surveys have shown that most of the CO emission comes from low-density, subthermally excited gas. The scaling laws derived from CO surveys (e.g., Dame et al. 1987; Scoville et al. 1987) give the mean H_2 density ranging from $n(H_2) = 73$ to 180 cm^{-3} for a giant molecular cloud of diameter 40 pc. For simplicity, we chose $n(H_2) = 10^2$ cm^{-3}, $T_k = 10$ K, and abundance ratio CO/$H_2 = 8 \times 10^{-5}$ for model calculations. In the parameter range of interest to us, a higher density slightly

decreases the intensity ratio $R_{\mathrm{C\,I/CO}}$, while a higher temperature increases the ratio.

Figure 6 shows the [C I]/CO intensity ratio $R_{\mathrm{C\,I/CO}}$ and the CO $J = 1$–0 excess brightness temperature calculated for a homogeneous cloud. The frequency distribution of the observed data weighted by the [C I] intensity is also superposed. A large amount of [C I] emission comes from gas with $N(\mathrm{CO})/dV = 10^{16}$–$10^{17}$ cm^{-2} (km s^{-1})$^{-1}$ and $\mathrm{C}^0/\mathrm{CO} = 2$–10. The [C I] optical depths are thin or moderate ($\tau_{\mathrm{C\,I}} \leq 5$) in the [C I]-emitting gas. The [C I] excitation temperature is typically 5–6 K. Note that a correction for the beam dilution effect gives a downward revision in the C^0/CO abundance ratio and an upward revision in the CO column density along isointensity-ratio curves. A beam filling factor can be estimated to be $f \gtrsim 0.5$ from a typical CO main-beam temperature in the [C I]-emitting region, $T_{\mathrm{MB}}(\mathrm{CO}) \sim 3$ K. Including these corrections, we can safely conclude that the [C I] emission from the Galactic disk is dominated by a population of neutral gas with high C^0/CO abundance ratios and moderate CO column densities. These conditions are found in clouds categorized as diffuse translucent clouds (e.g., Stark & van Dishoeck 1994; Ingalls et al. 1994, 1997). Different choices of the density and temperature within the range $n(\mathrm{H_2}) = 10^2$–10^3 cm^{-3} and $T_k = 10$–20 K do not alter this conclusion. Large-scale CO surveys implies that a significant amount of ^{12}CO emission in the Galactic plane is produced by molecular gas with a lower opacity than that of giant molecular clouds (Polk et al. 1988; Chiar et al. 1994). The [C I] emission in the Galactic plane is also produced by such "translucent" molecular clouds.

5.2. *Distribution of the Intensity Ratio*

5.2.1. *Radial Distributions*

The [C I] and CO data were converted to bulk emissivity assuming pure circular motion and axial symmetry of the gas distribution, following the precepts of Burton & Gordon (1978). The effective emissivity (Sanders et al. 1984; Bronfman et al. 1988), $J(l, b, V_{\mathrm{LSR}})$ (K km s^{-1} kpc^{-1}), is defined by

$$J(l, b, V_{\mathrm{LSR}}) = T_{\mathrm{MB}}(l, b, V_{\mathrm{LSR}}) \frac{dV}{ds}, \tag{1}$$

where s is the heliocentric distance and dV/ds is the velocity gradient along the line of sight. The bulk emissivity $J(r)$ was calculated as a function of the Galactocentric distance r by taking an average of the observed emissivity over concentric rings of thickness $\Delta R = 0.5$ kpc:

$$\begin{aligned} J(r) &= \sum_i J_i(l, b, V) w_i / \sum_i w_i \\ &= \begin{cases} \sum_i T_i(l, b, V) \dfrac{\Delta V}{\Delta s} w_i / \sum w_i, & r \geq r_\odot, \\ \sum_i T_i(l, b, V) \\ \times \left[\left(\dfrac{\Delta V}{\Delta s} w_i \right)_{\mathrm{near}} + \left(\dfrac{\Delta V}{\Delta s} w_i \right)_{\mathrm{far}} \right] \\ / \sum_i \left[(w_i)_{\mathrm{near}} + (w_i)_{\mathrm{far}} \right], & r < r_\odot, \end{cases} \end{aligned} \tag{2}$$

where Δs is the segment of a line of sight corresponding to ΔV and r, and w_i is the weight assigned to each datum. We took $w_i = \Delta s$. The uncertainty in the bulk emissivity is given by $[\Delta J(r)]^2 = \sum_i [\partial J(r)/\partial T_i]^2 (\Delta T)^2$, where ΔT is the uncertainty in the brightness temperature. The Galactocentric distance r was calculated from l and V_{LSR} by geometric consideration of the Galactic rotation. Inside the solar circle, two heliocentric distances are possible for a given Galactocentric distance. We adopt the analytical expression for the Galactic rotation curve employed by Brand & Blitz (1993),

$$\Theta(r)/\Theta_\odot = a_1 (r/r_\odot)^{a_2} + a_3, \tag{3}$$

where $\Theta(r)$ and $\Theta_\odot$ are, respectively, the rotation velocity at r and that at the solar circle. We force $\Theta(r_\odot) = \Theta_\odot$, implying $a_3 = 1 - a_1$, and thereby the independent parameters become a_1 and a_2. We employed $a_1 = 0.705$ and $a_2 = 0.35 \times 10^{-8}$ according to Russeil (2003).

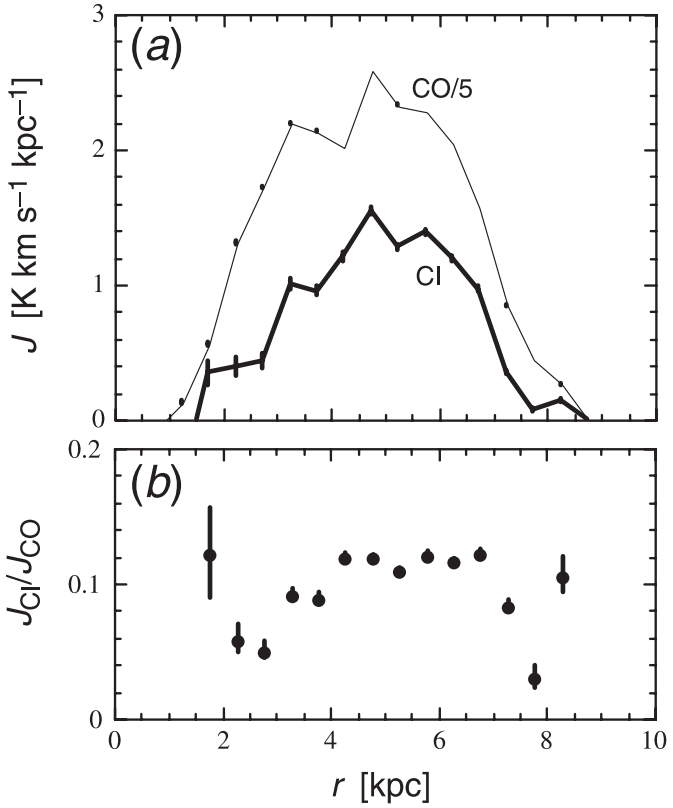

FIG. 7.—(*a*) Variation of bulk [C I] and CO emissivities with the galactocentric radius. (*b*) Ratio of bulk emissivities ($J_{\mathrm{C\,I}}/J_{\mathrm{CO}}$) across the Galactic disk. Errors are in 1 σ in both panels.

The [C I] and CO bulk emissivities and their ratio are presented in Figure 7. Errors are the standard deviation of the mean calculated from the uncertainty in bulk emissivity [$\Delta J(r)$]. A shape of the radial distribution of the [C I] bulk emissivity is in good agreement with that of CO, except for small bumps at $r \simeq 2$ and 8 kpc. Both emissivities display a broad peak at the "molecular ring" decreasing steeply toward the sides. The ratio of [C I] and CO bulk emissivities stays roughly constant ($\sim$0.12) at the molecular ring, $r = 4$–7 kpc. On either side of the molecular ring, the ratio decreases by a factor of 3 and then increases at the [C I] bumps. The inner bump in the [C I] radial distribution (Fig. 7*a*) is generated by the contribution of high [C I]/CO intensity ratio gas associated with the 3 kpc arm, which is an inner arm-like feature having large noncircular velocity. We should exclude this feature from consideration here, since it apparently breaks the assumption of axial symmetry. The outer bump is generated by a broad-velocity [C I] emission feature at $(l, V_{\mathrm{LSR}}) = (345^\circ, 10$ km s$^{-1})$, which may be a cloud from the near side of the Sagittarius-Carina spiral arm. We should take

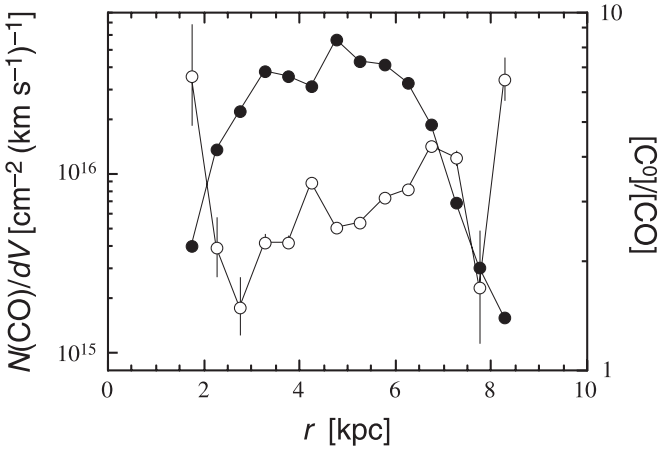

FIG. 8.—Plot of CO column density per unit velocity width (*filled circles, left axis*) and C^0/CO abundance (*open circles, right axis*) as a function of the galactocentric distance. $J/T_{MB} = 3$ and uniform brightness over each radius ring was assumed.

these bumps as a preliminary result only, since they do not have enough statistical significance.

We have a smooth radial trend in the [C I]/CO ratio across the Galactic disk, excluding the contribution of the [C I] bumps. What produces this Galactic trend? As we commented in § 5.1.2, the [C I]/CO intensity ratio $R_{C\,I/CO}$ is determined by the gas column density per velocity width and the C^0/CO abundance ratio. To separate these two factors we again refer to the LVG calculations. The definition of the bulk emissivity says that the emissivity is a measure of typical brightness temperature from a unit volume. Here we boldly assumed $J/T_{MB} = 3$, which corresponds to a volume filling factor of 0.3 with a typical velocity gradient $\Delta V/\Delta s = 10$ km s^{-1} kpc^{-1}, and obtained radial distributions of the column density and C^0/CO abundance ratio (Fig. 8). The C^0/CO abundance ratio shows a gradual increase from $r = 3$ to 7 kpc, while the column density shows a radial distribution similar to those of the [C I] and CO emissivities. A different choice of the J/T_{MB} ratio does not erase the trend, although it alters absolute values. This result indicates that the outer decline of the [C I]/CO ratio is due to the steep decline of the column density and that the inner decline is largely due to the monotonous decrease of the C^0/CO abundance ratio toward the Galactic center.

The mechanism responsible for the C^0/CO Galactic trend may be unrelated to the physical conditions, since no radial trend has been found in the physical conditions of molecular clouds across the Galactic disk (Liszt 1993; Hasegawa et al. 1998). Contribution of diffuse atomic gas in interarm regions may be rejected by a striking resemblance between the [C I] and CO *l-V* distributions. The determinant of the bulk C^0/CO abundance ratio must be deeply concerned to the formation and destructive processes of molecular clouds in the Galactic disk.

5.2.2. *Relation to the Spiral Arms*

It is widely accepted that the evolution of interstellar matter in the Galactic disk is greatly affected by encounters with the Galactic spiral arms. The *l-V* diagram of the [C I]/CO intensity ratio $R_{C\,I/CO} \equiv T_{MB}(C\,I)/T_{MB}(CO)$ (Fig. 9) may be useful to investigate the effect of spiral arms on neutral interstellar matter. The [C I] and CO data were smoothed to a 2 km s^{-1} resolution, and data with $T_{MB}(C\,I) < 0.25$ K were excluded to obtain a reliable distribution of the intensity ratio. Loci in *l-V* space of three major spiral arms, 3 kpc arms, and those of giant H II regions (Georgelin & Georgelin 1976) are also presented.

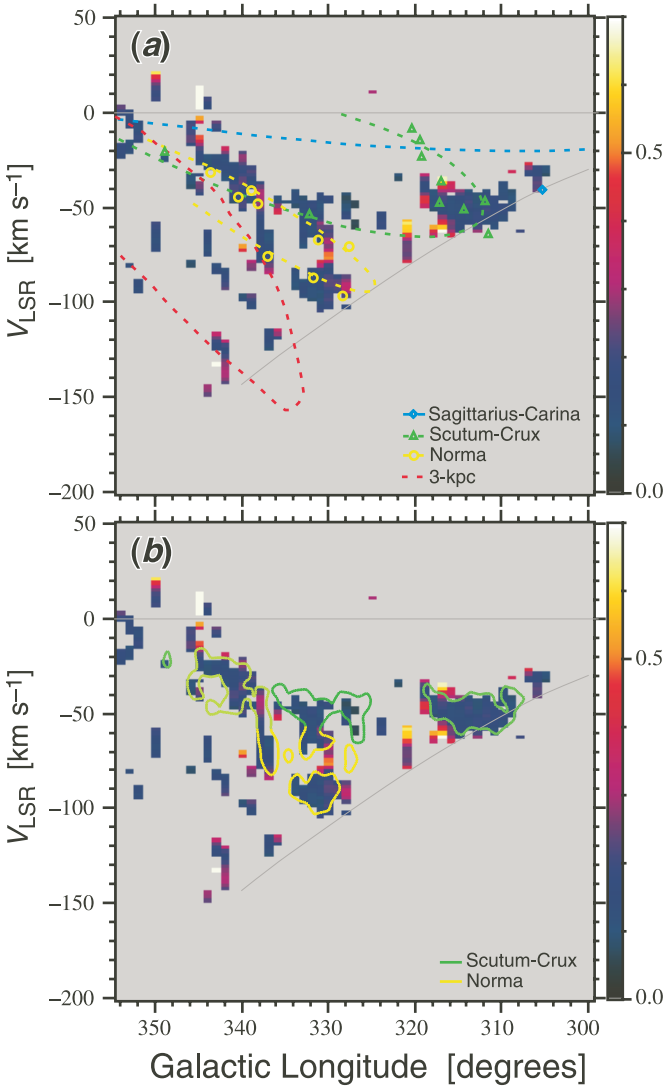

FIG. 9.—Longitude-velocity map of the antenna temperature ratio $R_{C\,I/CO}$; (*a*) with loci of the arms and of giant H II regions, and (*b*) with CO complexes that may be associated with the Scutum-Crux and Norma arms. Both data sets were smoothed to a 2 km s^{-1} resolution, and data with $T_{MB}(C\,I) < 0.25$ K were excluded. Thin gray lines show the zero velocity line and the terminal velocity line for $r \geq 3$ kpc.

We see several areas with high intensity ratios ($R_{C\,I/CO} > 0.3$). These high-ratio areas are not necessarily associated with the bright H II regions closely. The intensity ratio seems to be rather low ($R_{C\,I/CO} \lesssim 0.2$) at cloud complexes that may be associated with the Scutum-Crux and Norma arms. Gas associated with the 3 kpc arm have rather high intensity ratios. We see a very high ratio feature at $(l, V_{LSR}) = (345^\circ, 10$ km s$^{-1})$. This could only be in the preliminary data, or it could be one of the broad-velocity [C I] emission features, which were also found at $(l, V_{LSR}) = (321^\circ, -70$ km s$^{-1})$, $(350^\circ, 20$ km s$^{-1})$, and in the direction of M17 (M. Nagai et al. 2005, in preparation). Although the origin of these broad-velocity [C I] features is unknown, they could belong to a population of neutral interstellar matter that is previously unrecognized.

We also found two groups of high-ratio areas at $(l, V_{LSR}) =$ (316° to 319°, -64 to -30 km s^{-1}) and (328° to 331°, -90 to -66 km s^{-1}). The former area corresponds to the Galactic eastern periphery of a cloud complex near the Scutum-Crux (Centaurus) tangent (e.g., Englmaier & Gerhard 1999). The latter resides in a CO hollow being encircled by giant H II regions

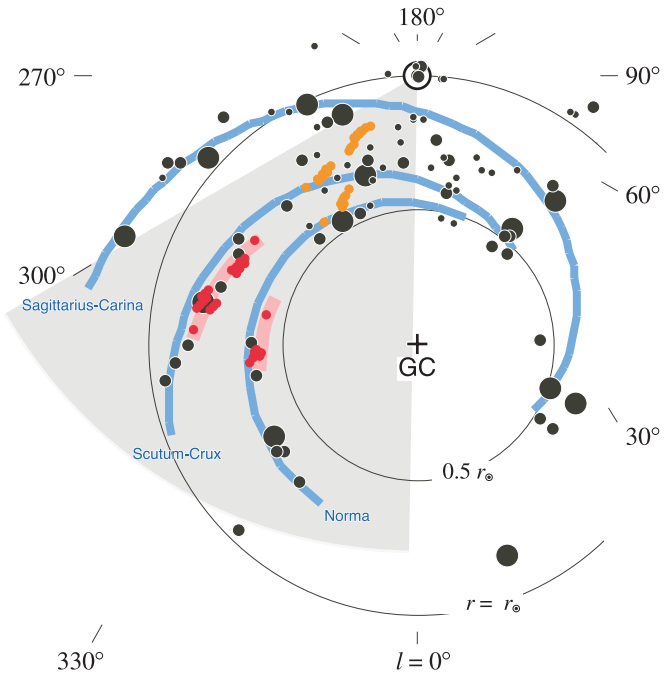

FIG. 10.—Three spiral arms of our Galaxy obtained by fitting logarithmic spirals to high-excitation parameter H II regions (*blue solid lines*). Loci of H II regions are shown by black filled circles with sizes representing the excitation classification of Georgelin & Georgelin (1976). The shaded area shows our survey coverage. Red and orange filled circles indicate positions of two groups of high [C I]/CO ratio areas ($R_{\rm C\,I/CO} > 0.3$) at their "far" and "near" kinematic distances, respectively. Thick pink lines show possible distributions of high-ratio gas.

associated with the Norma arm. These high ratios are likely due to the higher C^0/CO abundance ratio rather than to the higher column density, because these locations are displaced from centers of cloud complexes associated with spiral arms. The *l-V* tracks of the Scutum-Crux and Norma arms seem to run around these high-ratio areas, placing them several degrees inside of the tangential points ($l \simeq 313°$, $325°$). Although a spiral arm traced solely by giant H II regions may be controversial, we employ them since they trace a massive star formation "front" in the arm. These tracks are essentially consistent with recent models of the Galactic spiral structure (Vallée 2002; Russeil 2003) in longitudes of interest to us.

Figure 10 shows the face-on distribution of the high-ratio areas ($R_{\rm C\,I/CO} > 0.3$) in the longitude ranges $l = 316°$–$319°$ and $l = 328°$–$331°$. Since we could not resolve the kinematic distance ambiguity, both distances are drawn with different colors. The high-ratio areas at their "near" distances are mainly distributed in interarm zones within 5 kpc from the Sun, while those at the "far" distances closely follow the inside of the far side of the Scutum-Crux and Norma arms. Although there is no strong evidence to reject the "near" kinematic distances, absence of high-ratio gas in the other interarm *l-V* zones could be circumstantial evidence against the "near" distances. If these high ratios originate from some processes related to the spiral arms, many of these high-ratio regions are likely at their "far" distances being associated with the far side of the Scutum-Crux and Norma arms.

These locations of high-ratio gas at their far kinematic distances correspond to the "upper stream" of the spiral arms in terms of the Galactic rotation, if the rotation velocity of gas is faster than that of the Galactic spiral pattern at those radii. The classical value of the pattern speed is $\Omega_p \simeq 13.5$ km s^{-1} kpc^{-1} (Lin et al. 1969), which implies the corotation circle in the outer region of the Galaxy ($r_{\rm cr} = 15$–20 kpc). Recently, some authors reported the corotation close to the solar circle (Fernández et al. 2001; Mishurov et al. 2002). Within the corotation circle, the rotation velocity of gas is faster than that of the spiral pattern.

The concentration of the high C^0/CO ratio gas upstream of the spiral arms is consistent with the commonly accepted scenario of phase transition of interstellar matter crossing spiral arms; (1) accumulation of diffuse atomic gas by the encounter with a spiral arm, (2) molecular cloud formation, (3) massive star formation in molecular clouds, (4) ionization and dissipation of molecular gas by newly born massive stars. The observed configuration of the [C I]/CO intensity ratio with respect to the spiral arms may correspond to the transition from phase (1) into the early stage of phase (2). In fact, the spatial difference between the centers of spiral arms and the high-ratio areas corresponds to a time lag of several $\times 10^6$ yr, which is similar to the $C^0 \rightarrow$ CO conversion timescale (e.g., Suzuki et al. 1992; Oka et al. 2004).

In this context, the Galactic trend in the C^0/CO abundance ratio mentioned in § 5.2.1 can be attributed to the radial trend in the $C^0 \rightarrow$ CO conversion efficiency. It is likely that the metallicity gradient across the Galactic disk (e.g., Shaver et al. 1983; Martín-Hernández et al. 2002) generates the radial trend in the $C^0 \rightarrow$ CO conversion efficiency. The higher metallicity in the inner Galaxy may result in the lower gas-to-dust ratio, providing more efficient shielding afforded by dust particles against photodissociation of CO. This mechanism reduces the minimum gas column density to be accumulated to shield against ultraviolet photons and thereby increases the efficiency of $C^0 \rightarrow$ CO conversion at spiral arms in the inner Galaxy.

6. SUMMARY

The first Galactic plane survey in the 492 GHz fine-structure transition of neutral atomic carbon ($C^0\ ^3P_1$–$^3P_0$; [C I]) has been performed with the Portable 18 cm Submillimeter-wave Telescope. The survey covers the area from $l = 300°$ to $354°$ with a $1°$ sampling. The coarsely sampled longitude-velocity (*l-V*) map of [C I] was compared with that of CO generated from the Columbia Southern Survey data. The principal results of this study are summarized as follows.

1. The longitude-velocity distribution of [C I] emission closely resembles that of CO $J = 1$–0, which confirms a widespread distribution of atomic carbon on the Galactic scale.

2. The ratio of the antenna temperatures, $T_{\rm MB}$(C I)/$T_{\rm MB}$(CO), concentrates on the narrow range from 0.05 to 0.3. An LVG analysis showed that [C I] emission from the Galactic disk is dominated by a population of neutral gas with high C^0/CO abundance ratios and moderate CO column densities, which can be categorized as diffuse translucent clouds.

3. The ratio of total integrated intensities, $W_{\rm C\,I}/W_{\rm CO}$, was 0.105 ± 0.004. This is slightly lower than that obtained from the coarse-resolution data by *COBE*, suggesting that neutral gas with low [C I]/CO intensity ratios may be abundant in the midplane of the Galactic disk compared to that out of the plane.

4. The ratio of bulk emissivity, $J_{\rm C\,I}/J_{\rm CO}$, shows a systematic trend across the southern Galactic disk interior to the solar circle. LVG analyses revealed the bulk C^0/CO abundance ratio increasing with the Galactic radius. A mechanism related to kiloparsec-scale structure of the Galaxy, such as the metallicity gradient, may control the radial trend of the C^0/CO abundance.

5. Two groups of high [C I]/CO intensity ratio areas are found in the *l-V* loci several degrees inside of the tangential points of

the Scutum-Crux and Norma arms. These could be gas condensations just accumulated in the potential well of spiral arms and could be in the early stage of molecular cloud formation.

We thank all members of the ASTE team for all the support in the operation at Pampa la Bola. We also thank T. Noguchi for providing SIS mixer devices of excellent performance. We are grateful to T. M. Dame for providing the CO $J = 1–0$ data in FITS format. We thank Y. Sekimoto, H. Yoshida, and T. Hirota who played important roles in the design and development of the telescope system. K. Tatematsu and T. Kamba made contributions in developing the receiver system and in operating the telescope at Pampa la Bola. We also thank H. Ozeki for his support in optimizing the spectrometer. M. Iwata made great contributions in developing the telescope control software. K. Matsuo developed the IF amplifier unit of the telescope. This study is supported by Grant-in-Aid from the Ministry of Education, Culture, Sports, Science, and Technology (07CE2002, 11304010, 12740119, and 10291056). L. B. acknowledges support by FONDECYT grant 1010431 and from Chilean Center for Astrophysics FONDAP 15010003.

REFERENCES

Bitran, M., Alvarez, H., Bronfman, L., May, J., & Thaddeus, P. 1997, A&AS, 125, 99
Brand, J., & Blitz, L. 1993, A&A, 275, 67
Bronfman, L., Alvarez, H., Cohen, R. S., & Thaddeus, P. 1989, ApJS, 71, 481
Bronfman, L., Cohen, R. S., Alvarez, H., May, J., & Thaddeus, P. 1988, ApJ, 324, 248
Burton, W. B., & Gordon, M. A. 1978, A&A, 63, 7
Chiar, J. E., Kutner, M. L., Verter, F., & Leous, J. 1994, ApJ, 431, 658
Dame, T. M., Elmegreen, B. G., Cohen, R. S., & Thaddeus, P. 1986, ApJ, 305, 892
Dame, T. M., et al. 1987, ApJ, 322, 706
Englmaier, P., & Gerhard, O. 1999, MNRAS, 304, 512
Fernández, D., Figueras, F., & Torra, J. 2001, A&A, 372, 833
Georgelin, Y. M., & Georgelin, Y. P. 1976, A&A, 49, 57
Gerin, M., & Phillips, T. G. 2000, ApJ, 537, 644
Gordon, M. A., & Burton, W. B. 1976, ApJ, 208, 346
Hasegawa, T., et al. 1998, in IAU Symp. 184, The Central Regions of the Galaxy and Galaxies, ed. Y. Sofue (Dordrecht: Kluwer), 179
Ingalls, J. G., Bania, T. M., & Jackson, J. M. 1994, ApJ, 431, L139
Ingalls, J. G., Chamberlin, R. A., Bania, T. M., & Jackson, J. M. 1997, ApJ, 479, 296
Kamegai, K., et al. 2003, ApJ, 589, 378
Kennicutt, R. 1982, ApJ, 253, 101
Lin, C. C., Yuan, C., & Shu, F. H. 1969, ApJ, 155, 721
Linsky, J. L. 1973, Sol. Phys., 28, 409
Liszt, H. 1993, ApJ, 411, 720
Maezawa, H., et al. 1999, ApJ, 524, L129
Martín-Hernández, N. L., et al. 2002, A&A, 381, 606
Mishurov, Y. N., Lépine, J. R. D., & Acharova, I. A. 2002, ApJ, 571, L113
Mulder, W. A., & Liem, B. T. 1986, A&A, 157, 148
Ojha, R., et al. 2001, ApJ, 548, 253
Oka, T., Iwata, M., Maezawa, H., Ikeda, M., Ito, T., Kamegai, K., Sakai, T., & Yamamoto, S. 2004, ApJ, 602, 803
Oka, T., et al. 2001, ApJ, 558, 176
Polk, K. S., Knapp, G. R., Stark, A. A., & Wilson, R. W. 1988, ApJ, 332, 432
Russeil, D. 2003, A&A, 397, 133
Sanders, D. B., Scoville, N. Z., & Solomon, P. M. 1985, ApJ, 289, 373
Sanders, D. B., Solomon, P. M., & Scoville, N. Z. 1984, ApJ, 276, 182
Scoville, N. Z., Yun, M. S., Sanders, D. B., Clemens, D. P., & Waller, W. H. 1987, ApJS, 63, 821
Shaver, P. A., McGee, R. X., Newton, L. M., Danks, A. C., & Pottasch, S. R. 1983, MNRAS, 204, 53
Stark, A. A., Bally, J., Knapp, G. R., Krahnert, A., Penzias, A. A., & Wolson, R. W. 1987, in IAU Symp. 115, Star Forming Regions, ed. M. Peimbert & J. Jugaku (Dordrecht: Reidel), 495
Stark, R., & van Dishoeck, E. F. 1994, A&A, 286, L43
Suzuki, H., Yamamoto, S., Ohishi, M., Kaifu, N., Ishikawa, S., Hirahara, Y., & Takano, S. 1992, ApJ, 392, 551
Ulich, B. L., & Haas, R. W. 1976, ApJS, 30, 247
Vallée, J. P. 2002, ApJ, 566, 261
Wilson, R. W., Jefferts, K. B., & Penzias, A. A. 1970, ApJ, 161, L43